

Dynamic Modeling of Underwater Multi-Hull Vehicles

Roberta Ingrosso*, Daniela De Palma,^{id} Giulio Avanzini^{id} and Giovanni Indiveri^{id}

Department of Innovation Engineering, University of Salento, ISME node, Lecce, Italy
E-mails: daniela.depalma@unisalento.it, giulio.avanzini@unisalento.it,
giovanni.indiveri@unisalento.it

(Accepted October 26, 2019. First published online: November 25, 2019)

SUMMARY

This paper describes a modeling approach to compute the lumped parameter hydrodynamic derivative matrices of an underwater multi-hull vehicle. The vehicle, modeled as a multi-body underwater system and denoted as cluster, can be composed by heterogeneous bodies with known dynamic parameters, rigidly connected. The nonlinear dynamic equations of the cluster and its parameters are derived by means of a modular approach, based on the composition of single basic elements. The ultimate objective is to derive a mathematical description of the multi-hull system that captures its most significant dynamics allowing to design model-based motion controllers and navigation filters. The modular nature of the resulting model can be exploited, by example, when control reconfiguration is to be dealt with in the presence of (possibly multiple) failures. The numerical simulation of a hypothetical cluster is presented and discussed.

KEYWORDS: Autonomous underwater vehicle; Multi-body underwater systems; Hydrodynamic model.

1. Introduction

Remotely operated vehicles and autonomous underwater vehicles (AUVs) are increasingly applied in a number of offshore applications in order to improve operation efficiency and operator's safety. Among many other applications, intervention missions of underwater vehicles equipped with manipulators represent an important asset in many applicative scenarios such as rescue, oil and gas industry, underwater construction, security, etc.

Modeling of generic underwater vehicles has been extensively treated in¹ and² The challenge for a multi-body cluster is to describe the nonlinear dynamics of the cluster from the dynamics of individual elements.

With respect to traditional modeling methods, the major difficulties arise from constraints when robots are connected. Indeed lumped parameter dynamic models of marine robots include many coefficients (hydrodynamic derivatives) associated with hydrodynamic interactions as drag, lift, added mass, and buoyancy. These can be numerically estimated by computational fluid dynamic (CFD) methods or experimentally. A more recent approach³ combines analytical and semiempirical estimation (ASE) methods with a parameter estimator based on the extended Kalman filter. In particular, the ASE methods build on theoretical and numerical hydrodynamics and geometric models of submarine vehicles.

If a multi-body vehicle is built by composing in cluster rigid bodies with known dynamic parameters, the question arises on how to exploit such knowledge to estimate the dynamic parameters of the cluster. This is the main issue addressed in this paper. Note that the unknown model parameters

* Corresponding author. E-mail: roberta.ingrosso@unisalento.it

could be experimentally estimated either off line (as in⁴) or online (as in⁵). However, typical maneuvers of practical interest for underwater vehicles are generally poorly exciting, jeopardizing the use of online observers for accurate parameter estimation.

Multi-body dynamics for underwater applications has been investigated in multiple papers. Refs. [6, 7] used multi-body dynamics to model underwater cables. Multi-body dynamics methods for modeling underwater vehicles have been used in refs. [8–13]. Ref. [12] presents an approach to multi-body dynamics modeling of a “semi-submersible” system consisting of a surface towing vehicle, a tow cable, and a towfish. The towing vehicle and towfish are modeled using 6-degrees of freedom (DOF) rigid body dynamics. Given that the towing cable can experience large deformations and displacements, its dynamics are modeled using the Absolute Nodal Coordinate Formulation method.

In ref. [13], the multi-body dynamic modeling and analysis of an AUV with a Variant Buoyancy System is performed based on Kane’s dynamic equations, namely, generalized forces that contribute to dynamics are determined by Kane’s approach. Kane’s method offers advantages over Newton–Euler and Lagrange methods for the computation of multi-body dynamics. With the use of generalized forces, the need for examining interaction and constraint forces among bodies is eliminated. Also refs. [10, 11] present a methodology for dynamic modeling of multi-body systems using Kane’s dynamic equations. In ref. [8], the cooperative navigation and control problem for fleets of streamer-vehicle systems is considered; in particular, a dynamic simulation model for a coupled streamer-vehicle system is proposed based on Kane’s method. Ref. [9] investigates the dynamic modeling and control of an underwater vehicle-manipulator multi-body system on the basis of the Newton–Euler recursive algorithm.

Dynamic modeling of reconfigurable underwater systems has been also investigated in refs. [14–17]. Ref. [17] proposes a method that combines Kane’s equations with graph theory to model underwater self-reconfigurable robots. Whereas the modeling approach proposed in refs. [14–16] is based on an application of the Udwadia–Kalaba equation.¹⁸ The papers develop the equations of motion for a system composed of N rigidly connected robots based on the Udwadia–Kalaba formulation.¹⁸ This framework uses quasi-velocities to derive the constraints imposed by rigid connections.

A specific approach for the dynamic modeling of a multi-body underwater vehicle is proposed in the present paper, which tackles the problem of representing in compact form the dynamics of a cluster of N rigidly connected elements. The characteristics of each element of the cluster (including its hydrodynamic model) are assumed known. The approach appears particularly interesting when one considers the development of larger vehicles designed and built by linking several smaller ones. Such an approach, which is at the basis of some recent research programs,¹⁹ presents several advantages, provided that (i) a considerable degree of redundancy is obtained, which allows for an easily reconfigurable control system in case of failures and (ii) testing of a single, smaller size, prototype element of the cluster is not only easier but also significantly cheaper than building and testing a single, large size, vehicle.

Moreover, when larger vehicles are realized by means of a cluster of existing (and possibly already tested) robots, performance and suitability of the new design with respect to mission requirements can be easily estimated as soon as the dynamic model is available. The present paper offers a method that allows to perform such an analysis, before the vehicle is built, possibly comparing different geometric configurations.

The elements of the cluster are heterogeneous robots/bodies, which can be either actuated or not actuated. When the cluster is assumed to be rigid, it is possible to derive the net values of external actions (hydrodynamic forces and moments, total weight, and buoyancy) and control forces and moments from those derived for the individual robots, without the need of evaluating internal actions associated with the constraint forces induced by the cluster structure on its elements during the motion. Hence, a modular approach is here proposed that exploits the knowledge of the dynamic model of a single underwater vehicle to obtain a mathematical model for a cluster of underwater robots. The original contribution is related to the application of a systematic approach to the dynamic modeling of modular underwater robots.

The advantage of this approach with respect to the Udwadia–Kalaba formulation ref. [5] is the derivation of a dynamic–hydrodynamic model for the whole multi-body system considering the constraints imposed by the rigid connections only at a geometrical level, without the need for



Fig. 1. The H2020 ROBUST project UVMS (Underwater Vehicle Manipulator System) platform.

explicitly deriving constraint forces and moments. Indeed, the proposed approach allows expressing directly the motion of the cluster using a 6-DOF equation, rather than using a 6N-DOF vector of quasi-velocities as in refs. [14–16]. Moreover, with respect to the recursive Newton–Eulerian formulation used in ref. [9], the proposed approach allows to derive a closed-form multi-body dynamic model.

Preliminary results of this modeling approach were presented in refs. [20]. The methodology is here described in more detail and applied to a realistic test case, derived in the framework of the activities of the H2020 ROBUST project,¹⁹ where a similar configuration was built and is currently under test (see Fig. 1). Numerical simulations are presented and discussed for assessing the validity of the modeling approach.

The rest of the paper is organized as follows: Section 2 defines the notation and recalls the main tools for the transformation of generalized forces and moments. Section 3 presents the problem formulation and the description of the equation of motion for the cluster and the single k -th body. The cluster model is derived building on the knowledge of the single body models. Numerical results are reported in Section 4. Finally, concluding remarks are addressed in Section 5.

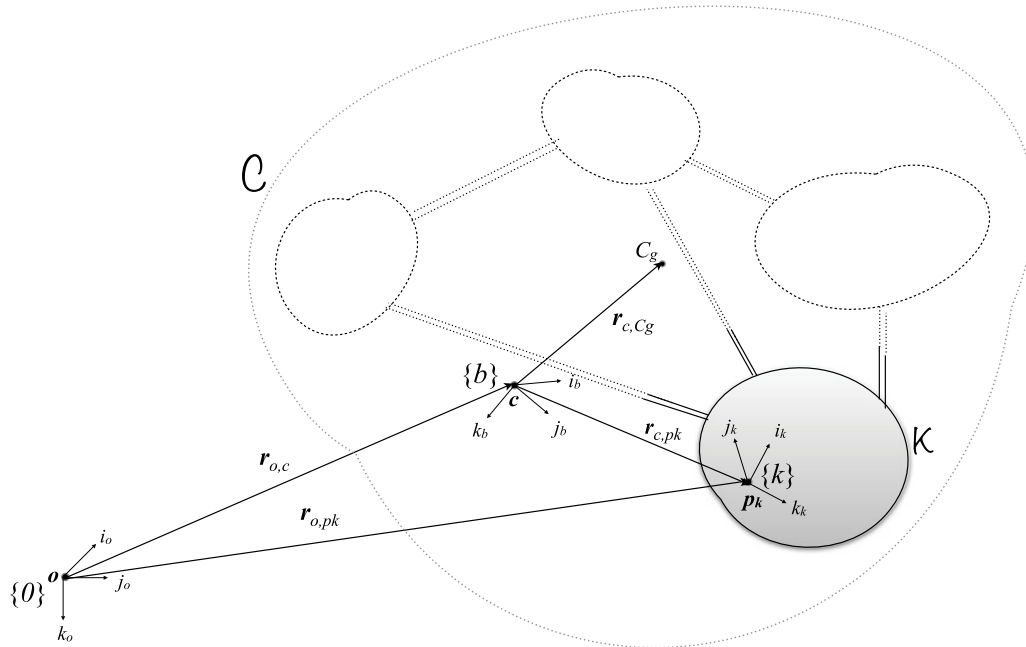


Fig. 2. Reference frames used for describing motion of cluster \mathcal{C} and k -th body \mathcal{K} linked rigidly.

2. Preliminaries and Notation

2.1. Clustering method

The clustering approach aims at providing a generic framework to model modular underwater vehicles. Let consider a generic multi-body rigid underwater vehicle, composed of N heterogeneous robots/bodies linked rigidly, denoted as cluster. Each element of the cluster can be either actuated or not actuated, and its characteristics (including its hydrodynamic parameters) are assumed known. The objective is to derive a mathematical description of the overall multi-body system dynamics building on the knowledge of the single basic elements. This dynamic modeling exploits a specific composition approach. It is based on the main assumption that the cluster is rigid. When the cluster is assumed to be rigid, it is possible to derive the net values of external actions (e.g., hydrodynamic forces and moments) and control forces and moments from those derived for the individual bodies, without the need of evaluating internal actions associated with the constraint forces induced by the cluster structure. However, it should be noted that, in line of principle, the distance among each single vehicle can influence the hydrodynamic forces and moments. If such a distance is sufficiently large, namely greater than two times the diameter of each single vehicle, the overall dynamic model will not significantly be affected by interference phenomena.

Note that when interference phenomena become significant, they will depend on the particular configuration considered, and either numerical CFD simulation or a dedicated experimental campaign are required for modeling hydrodynamic forces and moments developed on the specific cluster. Indeed, in what follows, the vehicles will be assumed to be at a distance such that the possible interferences can be neglected. The proposed clustering approach has the benefit to simplify the design of accurate controllers. This is an important feature, especially when control reconfiguration is to be dealt with in the presence of (possibly multiple) failures.

2.2. Notations

In order to describe the motion of multi-body generic rigid underwater vehicle by means of rigid body DOF, the reference frames, illustrated in Fig. 2, are defined as follows:

- $\{0\}$: inertial North-East-Down (NED) earth-fixed reference frame with origin in $o \in \mathbb{R}^3$;
- $\{b\}$: cluster-fixed reference frame with origin in $c \in \mathbb{R}^3$, where c is the point chosen as pole for forces and moments;

- $\{k\}$: k -th body-fixed reference frame ($k = 1, \dots, N$) with origin in a point $p_k \in \mathbb{R}^3$ of the k -th body, where p_k is the point chosen as pole for forces and moments.

Moreover, the following notation will be adopted for vectors in the coordinate systems $\{0\}$, $\{b\}$, and $\{k\}$:

- ${}^b\mathbf{r}_{c,p_k}$ = position vector from c to p_k expressed in frame $\{b\}$ where it is constant (rigid body constraint);
- ${}^0\mathbf{v}_{p_k/o}$ = linear velocity of p_k with respect to o expressed in $\{0\}$;
- ${}^b\boldsymbol{\omega}_{b/0}$ = angular velocity of $\{b\}$ with respect to $\{0\}$ expressed in $\{b\}$;
- ${}^b\mathbf{v}_{c/o}$ = generalized velocity of c with respect to o expressed in $\{b\}$;
- ${}^k\mathbf{f}$ = force with line of action through the point p_k expressed in $\{k\}$;
- ${}^b\mathbf{m}$ = moment about the point c expressed in $\{b\}$;
- ${}^0\boldsymbol{\eta}_b$ = Euler angles between $\{b\}$ and $\{0\}$;
- ${}^b\dot{\mathbf{v}}_{c/o} = \frac{d}{dt} {}^b\mathbf{v}_{c/o}$ time derivative of ${}^b\mathbf{v}_{c/o}$;
- C_g is the cluster center of gravity.

The symbol $S(\cdot) \in \mathbb{R}^{3 \times 3}$ denotes the skew symmetric matrix associated with the cross product, such that $S(\mathbf{a})\mathbf{b} = \mathbf{a} \times \mathbf{b}$ for any $\mathbf{a}, \mathbf{b} \in \mathbb{R}^{3 \times 3}$.

From Fig. 2 it follows that

$${}^0\mathbf{r}_{o,p_k} = {}^0\mathbf{r}_{o,c} + {}^0R_b {}^b\mathbf{r}_{c,p_k}, \tag{1}$$

where ${}^0R_b \in SO(3)$ is the rotation matrix between frame $\{b\}$ and $\{0\}$. Time differentiation of (1) gives the velocity of the point p_k (origin of k -th frame $\{k\}$) with respect to o (origin of frame $\{0\}$) expressed in $\{0\}$, that is:

$${}^0\mathbf{v}_{p_k/o} = \frac{d}{dt} {}^0\mathbf{r}_{o,p_k} = {}^0\mathbf{v}_{c/o} + {}^0\boldsymbol{\omega}_{b/0} \times {}^0\mathbf{r}_{c,p_k}. \tag{2}$$

From time differentiation of (2) it follows that:

$${}^0\mathbf{a}_{p_k/o} = \frac{d}{dt} {}^0\mathbf{v}_{c/o} + \left(\frac{d}{dt} {}^0\boldsymbol{\omega}_{b/0} \right) \times {}^0\mathbf{r}_{c,p_k} + {}^0\boldsymbol{\omega}_{b/0} \times ({}^0\boldsymbol{\omega}_{b/0} \times {}^0\mathbf{r}_{c,p_k}). \tag{3}$$

In the following, we recall the main tools for the transformation of the generalized forces and moments between two points in different reference frames.

2.3. Generalized velocity vectors in different reference frames

The generalized velocity of point p_k of the k -th body with respect to o expressed in $\{k\}$ is denoted as

$${}^k\mathbf{v}_{p_k/o} := \begin{bmatrix} {}^k\mathbf{v}_{p_k/o} \\ {}^k\boldsymbol{\omega}_{k/0} \end{bmatrix}. \tag{4}$$

In order to express the relation between ${}^k\mathbf{v}_{p_k/o}$ and ${}^b\mathbf{v}_{c/o}$, it is necessary first to all to express the vectors in the same reference frame $\{b\}$. Letting bR_k be the rotation matrix from $\{k\}$ to $\{b\}$, one has that:

$${}^b\mathbf{v}_{p_k/o} = \begin{bmatrix} {}^b\mathbf{v}_{p_k/o} \\ {}^b\boldsymbol{\omega}_{k/0} \end{bmatrix} = {}^b\bar{R}_k {}^k\mathbf{v}_{p_k/o}, \tag{5}$$

where matrix ${}^b\bar{R}_k \in SO(6)$ is defined as

$${}^b\bar{R}_k := \begin{bmatrix} {}^bR_k & 0_{3 \times 3} \\ 0_{3 \times 3} & {}^bR_k \end{bmatrix} \in \mathbb{R}^{6 \times 6}. \tag{6}$$

Note that since all points of a rigid body have the same angular velocity, the assumption of a rigid cluster implies that ${}^b\boldsymbol{\omega}_{k/o} = {}^b\boldsymbol{\omega}_{b/o}$. Now, as also illustrated in,² the transformation between ${}^b\mathbf{v}_{p_k/o}$ and ${}^b\mathbf{v}_{c/o}$ can be expressed as follows:

$${}^b\mathbf{v}_{p_k/o} = T({}^b\mathbf{r}_{c,p_k}) {}^b\mathbf{v}_{c/o}, \tag{7}$$

where the matrix $T({}^b\mathbf{r}_{c,p_k})$ is given by

$$T({}^b\mathbf{r}_{c,p_k}) = \begin{bmatrix} I_{3 \times 3} & -S({}^b\mathbf{r}_{c,p_k}) \\ \mathbf{0}_{3 \times 3} & I_{3 \times 3} \end{bmatrix}, \tag{8}$$

summarizing

$${}^k\mathbf{v}_{p_k/o} = {}^k\bar{R}_b T({}^b\mathbf{r}_{c,p_k}) {}^b\mathbf{v}_{c/o}. \tag{9}$$

Similarly it can be shown that time differentiating (5) leads to the following:

$${}^k\dot{\mathbf{v}}_{p_k/o} = {}^k\bar{R}_b T({}^b\mathbf{r}_{c,p_k}) {}^b\dot{\mathbf{v}}_{c/o}. \tag{10}$$

2.4. Generalized forces in different reference frames

Letting ${}^k_{p_k}\boldsymbol{\tau}_k$ be the generalized forces vector acting on k -th about p_k expressed in $\{k\}$

$${}^k_{p_k}\boldsymbol{\tau}_k = \begin{bmatrix} {}^k_{p_k}\mathbf{f}_k \\ {}^k_{p_k}\mathbf{m}_k \end{bmatrix} \tag{11}$$

the generalized forces can be expressed in the cluster-fixed reference frame $\{b\}$ using the matrix ${}^b\bar{R}_k$, previously defined:

$${}^b_{p_k}\boldsymbol{\tau}_k = {}^b\bar{R}_k {}^k_{p_k}\boldsymbol{\tau}_k. \tag{12}$$

As also illustrated in ref. [2], the transformation of the generalized forces between the points p_k and c in frame $\{b\}$ is given by

$${}^b_c\boldsymbol{\tau}_k = T^\top({}^b\mathbf{r}_{c,p_k}) {}^b_{p_k}\boldsymbol{\tau}_k. \tag{13}$$

Hence, the generalized forces about the point c expressed in $\{b\}$, that is, ${}^b_c\boldsymbol{\tau}_k$, can be written as a function of the generalized forces about the point p_k expressed in $\{k\}$ ${}^k_{p_k}\boldsymbol{\tau}_k$ through the following transformation:

$${}^b_c\boldsymbol{\tau}_k = T^\top({}^b\mathbf{r}_{c,p_k}) {}^b\bar{R}_k {}^k_{p_k}\boldsymbol{\tau}_k. \tag{14}$$

3. Cluster Equations of Motion

3.1. Kinematic equations

Assuming that the cluster of N robots is rigid, its 6-DOF kinematic equations can be expressed as follows:

$${}^0\dot{\mathbf{r}}_{o,c} = {}^0R_b {}^b\mathbf{v}_{c/o} \tag{15}$$

$${}^b\dot{R}_0 = -S({}^b\boldsymbol{\omega}_{b/o}) {}^bR_0, \tag{16}$$

where ${}^0\mathbf{r}_{o,c} = [x, y, z]^\top$ denotes the NED position of the cluster in frame $\{0\}$, ${}^b\mathbf{v}_{c/o} = [u, v, w]^\top$ and ${}^b\boldsymbol{\omega}_{b/o} = [p, q, r]^\top$ are the cluster-fixed linear and angular velocity vectors, respectively. So, Eq. (15) describes the translational motion and (16) describes the rotational motion (i.e., kinematics of the rotation matrix).

It is worth highlighting that the standard kinematic equations for the rotational motion used, for example, in refs. [2, 21], make use of the Euler angles as a parametrization of $SO(3)$. It is known that any minimal rotation matrix parametrization is singular. The formulation adopted in (16) has the advantage being derived without needing any specific parametrization of $SO(3)$, hence avoiding all the issues related to minimal representation singularities. Of course, if needed, Euler angles (${}^0\Phi_b$) could always be derived from the elements of the rotation matrix bR_0 as reported in ref. [22].

3.2. Dynamic equations

As shown in refs. [2, 23], the standard lumped parameter model used in most robotics applications is given by

$$M_{rb} \dot{b} \mathbf{v}_{c/o} + C_{rb} (b \mathbf{v}_{c/o}) b \mathbf{v}_{c/o} = b \boldsymbol{\tau}_{rb}. \tag{17}$$

Equation (17) represents the Newton–Euler dynamic equations of motion expressed in an arbitrary cluster-fixed coordinate frame, where

- $b \mathbf{v}_{c/o} := [b \mathbf{v}_{c/o}^\top \ b \boldsymbol{\omega}_{b/o}^\top]^\top$ is the cluster-fixed generalized (linear and angular) velocity vector,
- $b \boldsymbol{\tau}_{rb}$ is a generalized vector of external forces and moments,
- M_{rb} is the rigid-body inertia matrix,
- C_{rb} is the rigid-body Coriolis and centripetal matrix.

The generalized vector of external forces and moments $b \boldsymbol{\tau}_{rb}$ is given by:

$$b \boldsymbol{\tau}_{rb} = b \boldsymbol{\tau}_{dp} + b \boldsymbol{\tau}_{drag} + b \boldsymbol{\tau}_{rf} + b \boldsymbol{\tau}_E + b \boldsymbol{\tau} + b \boldsymbol{\tau}_L, \tag{18}$$

where

- $b \boldsymbol{\tau}_{dp}$ is the vector of dynamic pressure forces and moments;
- $b \boldsymbol{\tau}_{drag}$ is the vector of viscous drag effects forces and moments;
- $b \boldsymbol{\tau}_{rf}$ is the vector of restoring (gravitational and buoyancy) forces and moments;
- $b \boldsymbol{\tau}_E = b \boldsymbol{\tau}_{wave} + b \boldsymbol{\tau}_{wind}$ is the vector of environmental forces and moments on a rigid body (it will be considered negligible in the following);
- $b \boldsymbol{\tau}$ is the vector of propulsion forces and moments;
- $b \boldsymbol{\tau}_L$ is the vector of lifting forces and moments.

Note that hydrodynamic forces and moments acting on the cluster are due to added mass, drag, and lifting ($b \boldsymbol{\tau}_{dp}$, $b \boldsymbol{\tau}_{drag}$, and $b \boldsymbol{\tau}_L$), whereas the restoring forces and moments are due to weight and buoyancy ($b \boldsymbol{\tau}_{rf}$).

With regards to the left-hand side of Eq. (17), the rigid-body inertia matrix M_{rb} and the rigid-body Coriolis and centripetal matrix C_{rb} in (17) are defined as in ref. [23]:

$$M_{rb} := \begin{bmatrix} mI_{3 \times 3} & -mS(b \mathbf{r}_{c,C_g}) \\ mS(b \mathbf{r}_{c,C_g}) & I_c \end{bmatrix}, \quad C_{rb}(b \boldsymbol{\omega}_{b/o}) := \begin{bmatrix} mS(b \boldsymbol{\omega}_{b/o}) & -mS(b \boldsymbol{\omega}_{b/o}) S(b \mathbf{r}_{c,C_g}) \\ mS(b \mathbf{r}_{c,C_g}) S(b \boldsymbol{\omega}_{b/o}) & -S(I_c b \boldsymbol{\omega}_{b/o}) \end{bmatrix}, \tag{19}$$

where

- m is the total mass of the cluster;
- $b \mathbf{r}_{c,C_g}$ is the distance vector from c to C_g expressed in frame $\{b\}$;
- I_c is cluster inertia matrix about c (origin of frame $\{b\}$).

Assuming that the inertia I_{gk} of the k -th vehicle about its center of gravity is known, the matrix I_c can be computed by means of the Huygens–Steiner theorem. Namely, the contribution of each vehicle to the cluster inertia matrix about c is given by

$$I_{ck} = I_{gk} - m_k S^2(b \mathbf{r}_{c,C_{gk}}), \tag{20}$$

where m_k is the mass of the k -th vehicle and $b \mathbf{r}_{c,C_{gk}}$ is the distance vector from c to C_{gk} expressed in frame $\{b\}$. Hence,

$$I_c = \sum_{k=1}^N I_{ck}. \tag{21}$$

As for the right-hand side of Eq. (17), that is, the vector of external forces and moments, the hydrodynamic/hydrostatic parameters for the cluster form the knowledge of the hydrodynamic/hydrostatic parameters of each individual body. The same for the propulsion and lifting forces and moments. To this aim, we consider the equations of motion of each body as illustrated in the following section.

3.3. Equations of motion for the k -th body

The equations of motion of the generic k -th body can be modeled as in ref. [2], where the generalized velocities ${}^k\mathbf{v}_{p_k/o}$ and forces ${}^k\boldsymbol{\tau}_{rbk}$ of the generic k -th body are expressed in its body-fixed frame $\{k\}$ ($k = 1, \dots, N$):

$$M_{rbk} {}^k\dot{\mathbf{v}}_{p_k/o} + C_{rbk} ({}^k\mathbf{v}_{p_k/o}) {}^k\mathbf{v}_{p_k/o} = {}^k\boldsymbol{\tau}_{rbk}, \tag{22}$$

with

$${}^k\boldsymbol{\tau}_{rbk} = {}^k\boldsymbol{\tau}_{dpk} + {}^k\boldsymbol{\tau}_{dragk} + {}^k\boldsymbol{\tau}_{rfk} + {}^k\boldsymbol{\tau}_{Ek} + {}^k\boldsymbol{\tau}_k + {}^k\boldsymbol{\tau}_{Lk}. \tag{23}$$

By means of the matrices ${}^b\bar{\mathbf{R}}_k$ and $T({}^b\mathbf{r}_{c,p_k})$ defined, in Sections 2.3 and 2.4, it is possible to specify the inertia, damping, lifting, restoring, and propulsion (when present) forces of all bodies about a common point c in a common reference frame $\{b\}$ making use of the cluster generalized velocity ${}^b\mathbf{v}_{c/o}$ only. The details of such procedure are illustrated in the following subsections. Hence, the generalized external forces for the cluster in (18) can be obtained from the sum of the individual contributions properly transformed.

3.3.1. Hydrodynamic forces and moments. In general, a body moving in a fluid is subject to external forces and moments due to the interaction between its external surface and the fluid. These hydrodynamic forces and moments are proportional to the fluid density and depend on speed and acceleration of the body.

Added mass terms. The dynamic pressure forces and moments acting on the k -th vehicle expressed in its local body frame $\{k\}$ can be expressed in the form

$${}^k\boldsymbol{\tau}_{dpk} = -M_{A_k} \frac{d}{dt} {}^k\mathbf{v}_{p_k/o} - C_{A_k} ({}^k\mathbf{v}_{p_k/o}) {}^k\mathbf{v}_{p_k/o}. \tag{24}$$

As highlighted in Section 2.4, the actions can be projected in the cluster-fixed reference frame $\{b\}$ and the pole for moments can be moved from p_k to c . At the same time, under the transformations described in Section 2.3, it is possible to express the generalized velocity of the k -th vehicle ${}^k\mathbf{v}_{p_k/o}$ as a function of the generalized cluster velocity ${}^b\mathbf{v}_{c/o}$, leading to the following equation:

$${}^b\boldsymbol{\tau}_{dpk} = -T^\top ({}^b\mathbf{r}_{c,p_k}) \bar{M}_{A_k} T ({}^b\mathbf{r}_{c,p_k}) \frac{d}{dt} {}^b\mathbf{v}_{c/o} - T^\top ({}^b\mathbf{r}_{c,p_k}) \bar{C}_{A_k} ({}^b\mathbf{v}_{c/o}) T ({}^b\mathbf{r}_{c,p_k}) {}^b\mathbf{v}_{c/o}, \tag{25}$$

where

$$\bar{M}_{A_k} = {}^b\bar{\mathbf{R}}_k M_{A_k} {}^k\bar{\mathbf{R}}_b, \tag{26}$$

and

$$\bar{C}_{A_k} ({}^b\mathbf{v}_{c/o}) = \begin{bmatrix} S ({}^b\boldsymbol{\omega}_{b/0}) & 0_{3 \times 3} \\ S ({}^b\mathbf{v}_{c/o} + {}^b\boldsymbol{\omega}_{b/0} \times {}^b\mathbf{r}_{c,p_k}) & S ({}^b\boldsymbol{\omega}_{b/0}) \end{bmatrix} \bar{M}_{A_k}. \tag{27}$$

Details about the derivation of (25) are reported in Appendix A. Equation (25) highlights how the dynamic pressure forces and moments of the k -th vehicle about point c can be expressed in the cluster reference frame using cluster velocity ${}^b\mathbf{v}_{c/o}$ only.

Lifting and drag forces and moments. Hydrodynamic drag and lift forces are conventionally calculated in the flow frame $\{f_k\}$.²⁴ The flow frame is commonly used in aerodynamics to model lift, side, and drag forces. The flow frame is found by rotating the k -th body frame $\{k\}$ such that the resulting x axis becomes parallel to the freestream flow. In the flow frame, the x axis points directly into the relative flow, while the z axis remains in the vehicle symmetry plane, perpendicular to the x axis. The

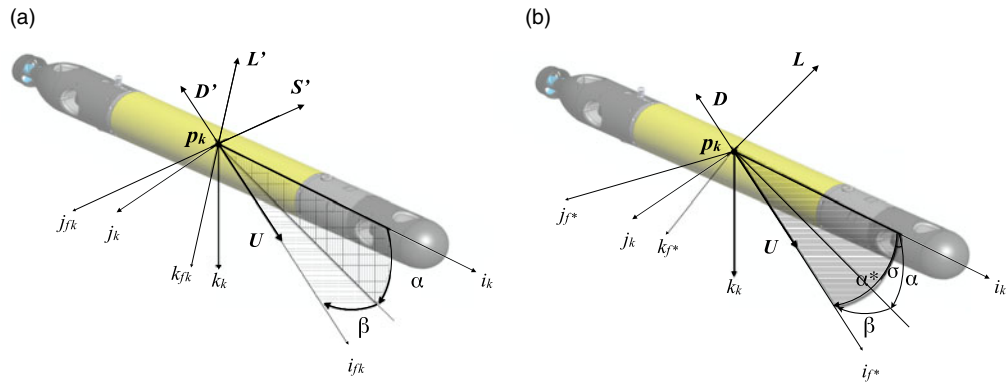


Fig. 3. (a): Flow frame $\{f_k\}$ as function of the angle of attack α and sideslip angle β (b): Alternative flow frame $\{f_k^*\}$ as function of the angle α^* and angle σ .

y axis completes the right-handed system. In the flow frame, each hydrodynamic term, lift, side, and drag resolve into a force that is parallel to one of the axes. Indeed, lift is, by definition, perpendicular to the relative flow, while drag is parallel and side force is lateral.

The transformation from flow to body frame is defined by two angles: the angle of attack α_k and the sideslip angle β_k . For the sake of notation compactness, in the following the subscript k and the angles α and β will be omitted.

For vehicles moving at a forward speed $U > 0$, the angle of attack and sideslip angle are equal to

$$\alpha = \tan^{-1}(w/u), \quad \beta = \sin^{-1}(v/U), \tag{28}$$

where $[u, v, w]$ are vehicle velocity components expressed in the body frame. The hydrodynamic forces in the flow frame ${}^{fk}f_a$ are expressed as: ${}^{fk}f_a = -[D' \ S' \ L']^\top$, where D' , S' , and L' denote the drag, side force, and lift, respectively, that are function of the angle of attack α .

Hydrodynamic force components are then projected into the body frame of the k -th vehicle by means of coordinate transformation matrix

$${}^kR_{fk} = \begin{bmatrix} \cos(\beta) \cos(\alpha) & -\sin(\beta) \cos(\alpha) & -\sin(\alpha) \\ \sin(\beta) & \cos(\beta) & 0 \\ \cos(\beta) \sin(\alpha) & -\sin(\beta) \sin(\alpha) & \cos(\alpha) \end{bmatrix}. \tag{29}$$

The determination of hydrodynamic force components D , S , and L requires an ad-hoc model, based on a database of hydrodynamic coefficients C_D , C_S , and C_L , such that each force component can be expressed as $0.5 \rho U^2 A C_j$, $j = D, S, L$, where ρ is fluid density and A a reference area. Each force coefficient depends on hydrodynamic angles, α and β , and Reynolds number $R_n = \rho V \ell / \mu$, where ℓ is a reference length and μ is fluid viscosity. Their values can be obtained experimentally or evaluated by means of CFD method, generating a database for various combinations of α and β . When a body is axisymmetric it is possible to take advantage of symmetry, provided that the plane which contains the symmetry axis of the body, x_B , and the velocity relative to the fluid is always a symmetry plane, hence, no side force in a direction perpendicular to this plane is expected. Only two hydrodynamic force components are necessary for determining the hydrodynamic action of the body, in a frame which has $x_f \equiv x_{f^*}$ and z_{f^*} as axes lying on this plane, as represented in Fig. 3(b).

This flow frame $\{f_k^*\}$ is obtained from the body frame with the following rotation matrix:

$${}^{f_k^*}R_k = R_{y,\alpha^*} R_{x,\sigma} = \begin{bmatrix} \cos(\alpha^*) & -\sin(\alpha^*) \cos(\sigma) & \sin(\alpha^*) \cos(\sigma) \\ 0 & \cos(\sigma) & \sin(\sigma) \\ -\sin(\alpha^*) & -\cos(\alpha^*) \sin(\sigma) & \cos(\alpha^*) \cos(\sigma) \end{bmatrix}. \tag{30}$$

The resulting flow frame $\{f_k^*\}$ is thus still aligned with the velocity vector relative to the flow, but symmetry of the body allows one to assume that $S = 0 \Rightarrow {}^{f_k^*}f_a = -[D \ 0 \ L]^\top$, where α^* and σ are equal to

$$\cos(\alpha^*) = \cos(\alpha) \cos(\beta), \quad \sin \sigma = \frac{\sin \beta}{\sin \alpha^*}. \tag{31}$$

The advantage of such a formulation is that we do not need to compute the lateral forces. Note that the D , S and L forces will be different from the forces D' , S' , and L' previously mentioned, because they will be computed making reference to the angle of attack α^* rather than α . Referring to the flow frame $\{f_k^*\}$, we can compute the norm of the lift force as:

$$L = \frac{1}{2} \rho U^2 A(\alpha^*) C_L(R_n, \alpha^*), \tag{32}$$

where $A(\alpha^*)$ is the projected frontal area of the body, and $C_L(R_n, \alpha^*)$ is the a-dimensional lift coefficient depending on the Reynolds number R_n and the angle of attack α^* . The lift coefficient is usually empirically determined. A good reference for experimental data is,²⁵ which contains a large amount of aerodynamic data from many different types of vehicles, wings, and other common engineering shapes. Usually the lift coefficient is assumed to depend only on the angle of attack, and independent of the Reynolds number, in the form:²⁶

$$C_L(R_n, \alpha^*) \simeq C_L(\alpha^*). \tag{33}$$

The lifting force consists of two different components due to circulation and cross-flow.²⁵ Within the range of small angles of attack, the linear circulation-type component of the lift is described by a lift coefficient linear with the angle of attack:

$$C_L = C_{L_{\alpha^*}} \alpha^*. \tag{34}$$

As the angle of attack increases, a nonlinear component of lift originates due to cross-flow; for example, for a cylinder the nonlinear lift coefficient is found to be:²⁵

$$C_L = C_c \sin^2(\alpha^*) \cos(\alpha^*), \tag{35}$$

being C_c a cross-flow coefficient. The lifting forces and moments in a flow frame centered in the k -th body center of pressure (cp_k) are ${}^{f_k^*}_{cp_k} \boldsymbol{\tau}_{L_k} = [0 \ 0 \ -L \ 0 \ 0 \ 0]^T$. Thus, the lifting forces and moments in the k -th body frame centered in p_k result in:

$${}^k_{p_k} \boldsymbol{\tau}_{L_k} = T^T ({}^k_{p_k, cp_k} \mathbf{r}_{cp_k}) {}^{f_k^*}_{cp_k} \boldsymbol{\tau}_{L_k}, \tag{36}$$

being \mathbf{r}_{cp_k, p_k} the distance vector from cp_k to p_k expressed in frame $\{k\}$. Of course, the lifting forces and moments can be expressed in the cluster-fixed frame $\{b\}$ and transported to the point c using the following transformation:

$${}^b_c \boldsymbol{\tau}_{L_k} = T^T ({}^b_{c, p_k} \mathbf{r}_{c, p_k}) {}^b_{p_k} {}^k_{p_k} \boldsymbol{\tau}_{L_k}. \tag{37}$$

With regards to the hydrodynamic damping, the drag forces of each k -th vehicle are parallel to the flow and can be expressed in its own body frame $\{k\}$ as in,²⁴ namely as the sum of a linear damping term (due to possible skin friction) and a nonlinear damping term (due to quadratic damping and higher-order terms) such that:

$${}^k_{p_k} \boldsymbol{\tau}_{drag_k} = -{}^k_{p_k} D_k ({}^k_{p_k/o} \mathbf{v}_{p_k/o}) {}^k_{p_k/o} \mathbf{v}_{p_k/o}, \tag{38}$$

where

$${}^k_{p_k} D_k ({}^k_{p_k/o} \mathbf{v}_{p_k/o}) = {}^k_{p_k} D_{k_{lin}} + {}^k_{p_k} D_{k_{quad}} ({}^k_{p_k/o} \mathbf{v}_{p_k/o}). \tag{39}$$

A first approximation of the damping matrix could be to assume that it is diagonal in the center of gravity,²⁴ that is:

$${}^k_{p_k} D_{k_{lin}} \approx -diag(X_u, Y_v, Z_w, K_p, M_q, N_r), \tag{40}$$

$${}^k_{p_k} D_{k_{quad}} ({}^k_{p_k/o} \mathbf{v}_{p_k/o}) \approx -diag(X_{u|u}|u|, Y_{v|v}|v|, Z_{w|w}|w|, K_{p|p}|p|, M_{q|q}|q|, N_{r|r}|r|). \tag{41}$$

Without loss of generality, here we have tacitly assumed that the k -th body frame is centered in the center of gravity. Yet, the absolute value of each velocity component ($|u|, |v|, |w|, |p|, |q|, |r|$) in (41) can be expressed as function of the cluster velocity ${}^b\mathbf{v}_{c/o}$:

$$\begin{aligned}
 \text{surge} : |u| &= |{}^k e_1^\top {}^k \mathbf{v}_{p_k/o}| = |{}^k e_1^\top {}^k \bar{\mathbf{R}}_b T({}^b \mathbf{r}_{c,p_k}) {}^b \mathbf{v}_{c/o}| \\
 \text{sway} : |v| &= |{}^k e_2^\top {}^k \mathbf{v}_{p_k/o}| = |{}^k e_2^\top {}^k \bar{\mathbf{R}}_b T({}^b \mathbf{r}_{c,p_k}) {}^b \mathbf{v}_{c/o}| \\
 \text{heave} : |w| &= |{}^k e_3^\top {}^k \mathbf{v}_{p_k/o}| = |{}^k e_3^\top {}^k \bar{\mathbf{R}}_b T({}^b \mathbf{r}_{c,p_k}) {}^b \mathbf{v}_{c/o}| \\
 \text{roll} : |p| &= |{}^k e_4^\top {}^k \mathbf{v}_{p_k/o}| = |{}^k e_4^\top {}^k \bar{\mathbf{R}}_b T({}^b \mathbf{r}_{c,p_k}) {}^b \mathbf{v}_{c/o}| \\
 \text{pitch} : |q| &= |{}^k e_5^\top {}^k \mathbf{v}_{p_k/o}| = |{}^k e_5^\top {}^k \bar{\mathbf{R}}_b T({}^b \mathbf{r}_{c,p_k}) {}^b \mathbf{v}_{c/o}| \\
 \text{yaw} : |r| &= |{}^k e_6^\top {}^k \mathbf{v}_{p_k/o}| = |{}^k e_6^\top {}^k \bar{\mathbf{R}}_b T({}^b \mathbf{r}_{c,p_k}) {}^b \mathbf{v}_{c/o}|,
 \end{aligned} \tag{42}$$

being $\{{}^k e_i; i = 1, \dots, 6\}$ the versors of the six-dimensional space \mathbb{R}^6 . At this point, following the procedure illustrated in 2.4, the damping forces ${}^k \boldsymbol{\tau}_{dragk}$ can be expressed in the frame $\{b\}$ and transformed to the point c , leading to:

$${}^b_c \boldsymbol{\tau}_{dragk} = -T^\top({}^b \mathbf{r}_{c,p_k}) {}^b_{p_k} \bar{\mathbf{D}}_k({}^b \mathbf{v}_{c/o}) T({}^b \mathbf{r}_{c,p_k}) {}^b \mathbf{v}_{c/o}, \tag{43}$$

where ${}^b_{p_k} \bar{\mathbf{D}}_k({}^b \mathbf{v}_{c/o})$ is defined as:

$${}^b_{p_k} \bar{\mathbf{D}}_k({}^b \mathbf{v}_{c/o}) = {}^b \bar{\mathbf{R}}_k {}^k D({}^b \mathbf{v}_{c/o}) {}^k \bar{\mathbf{R}}_b^b. \tag{44}$$

Mathematical details about the derivation of (43) are reported in Appendix B.

3.3.2. *Hydrostatic forces and moments.* The restoring terms are determined by the gravitational and buoyancy forces and are expressed as:²⁴

$${}^k_{p_k} \boldsymbol{\tau}_{rfk} = \begin{bmatrix} {}^k \mathbf{f}_{rfk} \\ {}^k \mathbf{m}_{rfk} \end{bmatrix} = - \begin{bmatrix} {}^k \mathbf{f}_{G_k} + {}^k \mathbf{f}_{B_k} \\ S({}^k \mathbf{r}_g) {}^k \mathbf{f}_{G_k} + S({}^k \mathbf{r}_B) {}^k \mathbf{f}_{B_k} \end{bmatrix}, \tag{45}$$

with ${}^k \mathbf{f}_{G_k}$ denoting the k -th vehicle gravitational forces and ${}^k \mathbf{f}_{B_k}$ the k -th vehicle buoyant forces, defined respectively as:

$${}^k \mathbf{f}_{G_k} = {}^k R_0 \begin{bmatrix} 0 \\ 0 \\ m_k g \end{bmatrix}, \quad {}^k \mathbf{f}_{B_k} = -{}^k R_0 \begin{bmatrix} 0 \\ 0 \\ \rho g \nabla_k \end{bmatrix},$$

where

- m_k is the k -th vehicle mass;
- g is the gravity constant;
- ρ is the fluid density (salt water);
- ∇_k is the displaced water volume of the k -th vehicle;
- ${}^k \mathbf{r}_g$ is the position vector of center of gravity C_{gk} of the k -th vehicle with respect to p_k (origin of body frame $\{k\}$);
- ${}^k \mathbf{r}_B$ is the position vector of center of buoyancy C_{bk} of the k -th vehicle with respect to p_k (origin of body frame $\{k\}$).

Again, using the usual procedure, ${}^k_{p_k} \boldsymbol{\tau}_{rfk}$ can be expressed in frame $\{b\}$ and transported about the point c (origin of frame $\{b\}$):

$${}^b_c \boldsymbol{\tau}_{rfk} = T^\top({}^b \mathbf{r}_{c,p_k}) {}^b_{p_k} \bar{\mathbf{R}}_k {}^k_{p_k} \boldsymbol{\tau}_{rfk}. \tag{46}$$

3.3.3. *Propulsion terms.* Assuming that the k -th vehicle has n_t thrusters, the propulsion forces and moments are expressed as

$${}^k_{p_k} \boldsymbol{\tau}_k := \mathbf{B}_k \mathbf{u}_k, \tag{47}$$

where $B_k \in \mathbb{R}^{6 \times n_k}$ is the allocation matrix and $\mathbf{u}_k \in \mathbb{R}^{n_k \times 1}$ is the thruster input vector.

Hence, when the propulsion forces and moments of the k -th vehicle are expressed in the cluster-fixed frame $\{b\}$ and the pole for moments moved from p_k to c became one has

$${}^b_c \boldsymbol{\tau}_k = T^\top ({}^b \mathbf{r}_{c,p_k}) {}^b \bar{R}_k {}^k \boldsymbol{\tau}_k. \tag{48}$$

Letting $B_k^* = T^\top ({}^b \mathbf{r}_{c,p_k}) {}^b \bar{R}_k B_k$, Eq. (48) can be expressed in compact form as

$${}^b_c \boldsymbol{\tau}_k = B_k^* \mathbf{u}_k. \tag{49}$$

3.4. Cluster 6-DOF dynamic model

In this section, a model for the cluster is derived on the basis of the knowledge of the inertial, hydrostatic, hydrodynamic, and propulsion actions for each single body. As already highlighted in the previous section, the inertia, lifting, damping, restoring, and propulsion forces (when present) of all bodies can be expressed in a common reference frame $\{b\}$ making use of the cluster velocity $\mathbf{v}_{c/o}$ only. This allows to specify the generalized vector of external forces for the cluster in Eq. (17) as the sum of the individual contributions of the N rigidly connected heterogeneous robots/bodies, that is

$$M_{rb} {}^b \dot{\mathbf{v}}_{c/o} + C_{rb} ({}^b \mathbf{v}_{c/o}) {}^b \mathbf{v}_{c/o} = \sum_{k=1}^N ({}^b_c \boldsymbol{\tau}_{dp_k} + {}^b_c \boldsymbol{\tau}_{drag_k} + {}^b_c \boldsymbol{\tau}_{rf_k} + {}^b_c \boldsymbol{\tau}_k + {}^b_c \boldsymbol{\tau}_{L_k}). \tag{50}$$

Interestingly, the contribution given by the propulsion forces and moments ${}^b_c \boldsymbol{\tau} = \sum_{k=1}^N {}^b_c \boldsymbol{\tau}_k$ can be rewritten as

$${}^b_c \boldsymbol{\tau} = B_{cl} \mathbf{U}, \tag{51}$$

with $B_{cl} = [B_1^* \dots B_N^*]$ and $\mathbf{U} = [\mathbf{u}_1 \dots \mathbf{u}_N]^\top$. As a result, the effects of the control input of each actuated robot are directly mapped onto the cluster frame and determine its motion. Summarizing the dynamics of the cluster is described by (52):

$$\begin{aligned} & (M_{rb} + M_{Acl}) {}^b \dot{\mathbf{v}}_{c/o} + (C_{rb} ({}^b \mathbf{v}_{c/o}) + C_{Acl} ({}^b \mathbf{v}_{c/o})) {}^b \mathbf{v}_{c/o} + \\ & + (D_{lcl} + D_{qcl} ({}^b \mathbf{v}_{c/o})) {}^b \mathbf{v}_{c/o} + \boldsymbol{\tau}_{rfcl} + \boldsymbol{\tau}_{Lcl} = B_{cl} \mathbf{U}, \end{aligned} \tag{52}$$

where the terms M_{Acl} , C_{Acl} , D_{lincl} , D_{quadcl} , $\boldsymbol{\tau}_{rfcl}$, $\boldsymbol{\tau}_{Lcl}$, and B_{cl} are recalled in Table I.

The advantage of this approach with respect to the Udwadia–Kalaba formulation¹⁸ is the derivation of a dynamic–hydrodynamic model for the whole multi-body system considering the constraints imposed by the rigid connections only at a geometrical level, without the need for explicitly deriving constraint forces and moments. Hence, the proposed approach allows expressing directly the motion of the cluster using the 6-DOF equation (52), rather than using a 6N-DOF vector of quasi-velocities as in.¹⁶ Moreover, the use of the cluster allocation matrix B_{cl} has the benefit of directly mapping the control input of each actuated robot on the cluster motion. This is an important feature, because it simplifies the design of dynamic controllers for the overall system especially when control reconfiguration it to be dealt with in the presence of (possibly multiple) actuator failures.

Remark. Following the approach discussed in,²³ if the vehicle moves inside a current, it is still possible to represent its dynamics by means of Eq. (52), under the assumption of an irrotational and constant flow field in NED frame. In this framework, the generalized velocity of the vehicle with respect to an inertial frame is given by $\mathbf{v}_{c/o} = \mathbf{v}_{c/ff} + \mathbf{v}_{f/o}$, where $\mathbf{v}_{c/ff} = [\mathbf{v}_{c/ff}^\top, \boldsymbol{\omega}_{c/ff}^\top]^\top$ is the generalized cluster’s velocity with respect to the fluid, whereas $\mathbf{v}_{f/o} = [\mathbf{v}_{f/o}^\top, \mathbf{0}_{3 \times 1}^\top]^\top$ is the generalized velocity of the current. It is sufficient to replace $\mathbf{v}_{c/o}$ with $\mathbf{v}_{c/ff}$ in Eq. (52) and let $\mathbf{v}_{c/o} = \mathbf{v}_{c/ff} + \mathbf{v}_{f/o}$ in Eq. (15).

4. Numerical Example

4.1. Test case

In order to numerically assess it, the proposed approach is applied to a hypothetical cluster composed by four AUVs connected by rigid rods, as illustrated in Fig. 4. Such a kind of configuration

Table I. Inertia, hydrodynamic, hydrostatic, and propulsion parameters for the single body and the cluster system.

	k^{th} body $k=1\dots N$	Cluster
Added mass terms	M_{A_k} $C_{A_k}({}^k\mathbf{v}_{p_k/o})$	$M_{Acl} = \sum_{k=1}^N (T^\top({}^b\mathbf{r}_{c,p_k}) \bar{M}_{A_k} T({}^b\mathbf{r}_{c,p_k}))$ $C_{Acl}({}^b\mathbf{v}_{c/o}) = \sum_{k=1}^N T^\top({}^b\mathbf{r}_{c,p_k}) \bar{C}_{A_k}({}^b\mathbf{v}_{c/o}) T({}^b\mathbf{r}_{c,p_k})$
Damping terms	${}^k_{p_k} D_{k_l}$ ${}^k_{p_k} D_{k_q}({}^k\mathbf{v}_{p_k/o})$	$D_{lcl} = \sum_{k=1}^N (T^\top({}^b\mathbf{r}_{c,p_k}) {}^b\bar{R}_k {}^k D_{k_l} {}^k\bar{R}_b T({}^b\mathbf{r}_{c,p_k}))$ $D_{qcl}({}^b\mathbf{v}_{c/o}) = \sum_{k=1}^N (T^\top({}^b\mathbf{r}_{c,p_k}) {}^b\bar{R}_k {}^k D_{k_q}({}^k\mathbf{v}_{p_k/o}) {}^k\bar{R}_b T({}^b\mathbf{r}_{c,p_k}))$
Lifting terms	${}^k_{p_k} \boldsymbol{\tau}_{L_k}$	$\boldsymbol{\tau}_{Lcl} = \sum_{k=1}^N (T^\top({}^b\mathbf{r}_{c,p_k}) {}^b\bar{R}_k {}^k \boldsymbol{\tau}_{L_k})$
Restoring terms	${}^k_{p_k} \boldsymbol{\tau}_{r_{f_k}}$	$\boldsymbol{\tau}_{r_{fcl}} = \sum_{k=1}^N (T^\top({}^b\mathbf{r}_{c,p_k}) {}^b\bar{R}_k {}^k \boldsymbol{\tau}_{r_{f_k}})$
Propulsion terms	B_k	$B_{cl} = [B_1^* \dots B_N^*]$

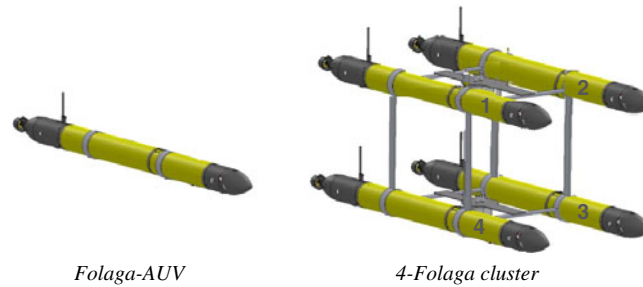


Fig. 4. 4-Folaga cluster multi-hull system obtained from single-vehicle Folaga-AUV.

is interesting from a practical point of view because the internal framework can serve as supporting infrastructure for payload modules, such as robotic manipulators, sensing, processing, or communication equipment typically necessary for the execution of specific missions.

The AUVs which compose the cluster are assumed to be *Folaga-AUV* type,²⁷ which model is available from the literature.²⁸ The connecting rods are assumed massless in the simulation, so that their contribution to mass properties, resorting, and hydrodynamic forces is neglected, for the sake of simplicity. Note that, in the presence of information on geometry and mass of the connecting rods, each one of them would simply represent an additional non-actuated element of the cluster. Hence, the validity of the modeling approach is not affected by this simplifying assumption.

A numerical simulator has been developed implementing the described modeling approach, and it is applied to the cluster depicted in Fig. 4. Several simulations are performed in both conditions, ideal (without environmental disturbances) and more realistic including ocean currents.

The mass and dimensions of AUV and cluster are reported in Table II, whereas added mass coefficients and linear drag coefficients of AUV and cluster are compared in Tables III and IV, respectively. Such terms depend on the shape of the body and are independent of velocity ${}^b\mathbf{v}_{c/o}$.

The other hydrodynamic coefficients depend on vehicle trajectory. Indeed, the quadratic drag and lift coefficients depend on the vehicle velocity, that is, ${}^b\mathbf{v}_{c/o}$ for the cluster and ${}^k\mathbf{v}_{p_k/o}$ for the single k -th *Folaga-AUV*. Fig. 5 reports the evolution of the lift coefficient as a function of the angle of attack for a single *Folaga-AUV*. The restoring coefficients depend on the actual orientation of the vehicle. Therefore, the effects of these contributions are compared making reference to a specific trajectory.

Table II. Mass and dimensions of *Folaga-AUV* single-body versus *4-Folaga cluster*.

Parameter	AUV	Cluster	Units
mass	25	100	kg
Width	1.882	1.882	m
Height	0.155	1.31	m
Length	0.155	1.31	m

Table III. Added mass coefficients of *Folaga-AUV* single-body versus *4-Folaga cluster*.

Coefficient	AUV	Cluster	Units
$X_{\dot{u}}$	0.47	1.88	kg
$Y_{\dot{v}}$	22.7	90.80	kg
$Z_{\dot{w}}$	22.7	90.80	kg
$K_{\dot{p}}$	0.1	45.8	kg m ²
$M_{\dot{q}}$	3.64	15.03	kg m ²
$N_{\dot{r}}$	3.64	15.03	kg m ²

Table IV. Linear drag coefficients of *Folaga-AUV* single-body versus *4-Folaga cluster*.

Coefficient	AUV	Cluster	Units
X_u	1.08	4.31	kg/s
Y_v	10.21	40.84	kg/s
Z_w	10.21	40.84	kg/s
K_p	$3 \cdot 10^{-3}$	20.42	kg m ² /s
M_q	1.06	5.32	kg m ² /s
N_r	1.06	5.32	kg m ² /s

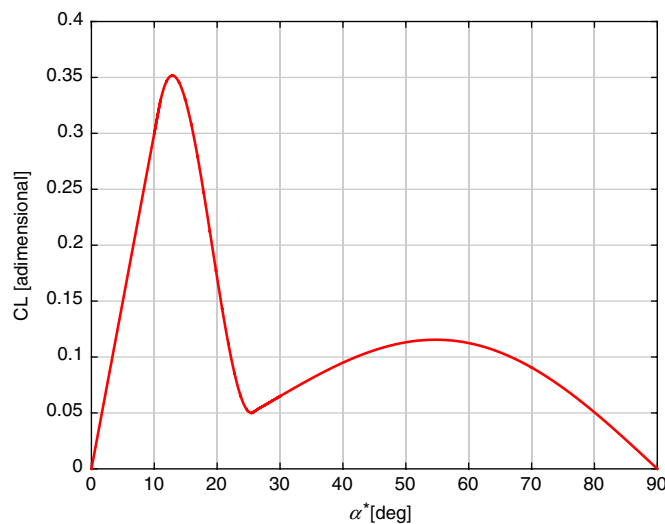


Fig. 5. Lift coefficient versus generic α^* ($0 - 90^\circ$) with Reynolds number $1.5 \cdot 10^5 \leq R_n \leq 1.5 \cdot 10^6$ for *Folaga-AUV*.

It is worth noting that cluster coefficients are not a bare sum of the individual contributions, but they are composed through the transformation matrix T defined in (8). This could result in cluster coefficients much higher than the individual AUV counterparts. This is particularly evident for roll drag moment (see Table IV), which appears to be four orders of magnitude greater than the individual AUV roll drag moment. The physical reason is that the individual AUVs roll drag moments are not

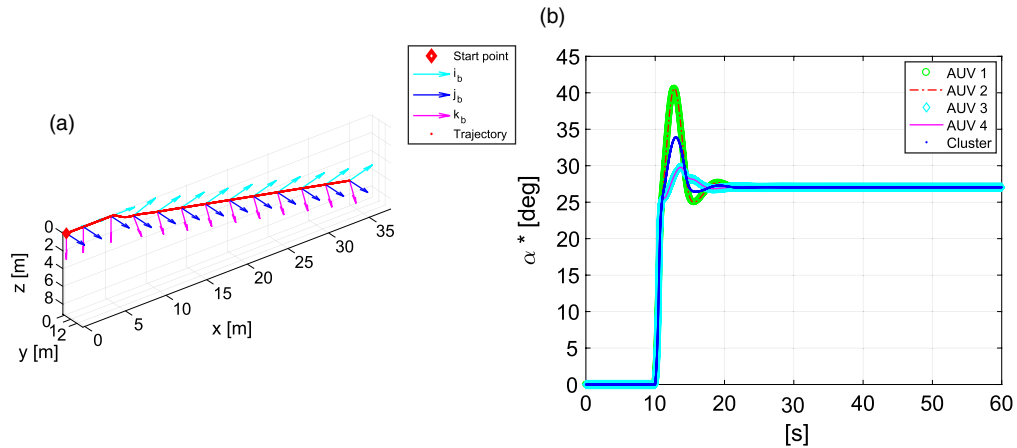


Fig. 6. (a) Trajectory of the 4-Folaga cluster. (b) Evolution of the angle of attack α^* of the 4-Folaga cluster system and the four Folaga-AUVs while performing the trajectory.

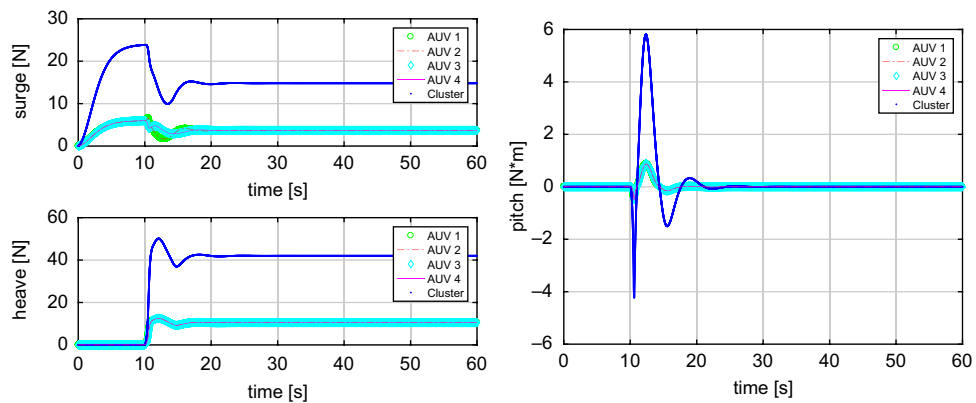


Fig. 7. Drag forces and moments of the 4 Folaga cluster system and the four Folaga-AUVs while performing trajectory in Fig. 6.

the only contributions to the cluster roll drag moment. Heave and sway linear drag forces acting on the single AUVs also generate a roll moment on the cluster. The magnitude of each contribution thus depends on the geometrical arrangement of the AUVs within the cluster.

4.2. Simulations

Two different experiments are considered. The first one, denoted as experiment 1, is a motion in the $\{x, z\}$ plane performed at zero sideslip angle, which is generated by activating the rear main thruster first (to accelerate the vehicle in the surge direction) and then the vertical thrusters of all AUVs with the same intensity (thus accelerating the vehicle in the heave direction). The second experiment, depicted in Fig. 10(a), is characterized by a not null sideslip angle. The motion is generated by activating the rear main thruster first (as in the previous example, to accelerate the vehicle in the surge direction) and then the lateral thrusters of each AUV with the same intensity.

Experiment 1. The first experiment is performed in the absence of environmental disturbances, and the resulting trajectory is reported in red in Fig. 6(a). The blue arrows represent the attitude of the body frame $\{i_b, j_b, k_b\}$ associated with the cluster. Fig. 6(b) represents the variation of the angle of attack, whereas Fig. 7 reports the evolution of the not null drag force components and moments for the cluster and the four AUVs, respectively, each one expressed in its own body frame. Fig. 8 reports the evolution of the not null lift forces and moments for the cluster system and the four AUVs, respectively. Finally, Fig. 9 shows the vehicle attitude and the not null restoring contributions.

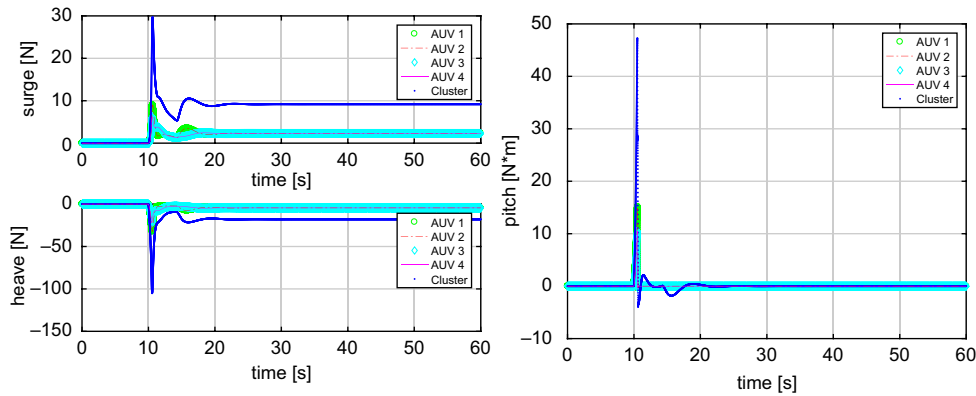


Fig. 8. Lift forces and moments of the 4-Folaga cluster system and the four-Folaga-AUVs while performing trajectory in Fig. 6.

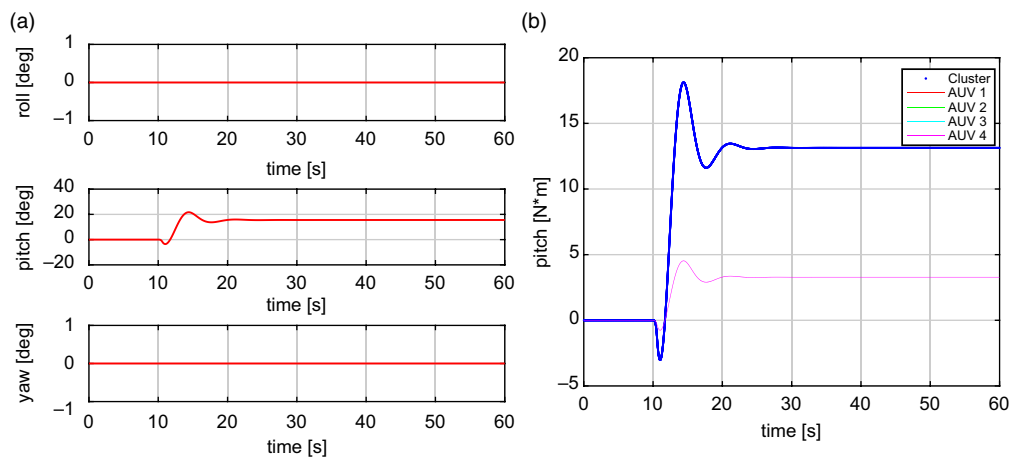


Fig. 9. (a) Attitude of the 4-Folaga cluster system while performing trajectory in Fig. 6. (b) Pitch restoring of the 4-Folaga cluster system and the four-Folaga-AUVs while performing trajectory in Fig. 6.

From Fig. 7 and 8, it is evident how the drag and lift forces evolution of cluster are the sum of the drag and lift forces one of the four AUVs. This is due to the geometrical composition of cluster model and to the similar physical conditions of each-Folaga-AUV. Of course, the lift forces depend also on the angle of attack α^* illustrated in Fig. 6(b). As expected, in correspondence of small angles of attack there is a pitch lift moment. Moreover, a further contribution to the pitch moment is generated by restoring torques, which for this purely longitudinal maneuver, in the absence of ocean currents, are zero around the other two axes.

The trajectory appears reasonable and the variation of state variables consistent with the expected behavior of the vehicle under the considered control action. Note that the vehicle achieves a steady descent trajectory, with constant angle of attack, provided that in the present longitudinal example $\alpha \equiv \alpha^*$.

Experiment 2. The second experiment is performed in both ideal conditions (without environmental disturbances) and more realistic ones including ocean currents. With reference to the ideal conditions case, the resulting trajectory is reported in red in Fig. 10(a). Figure 10(b) provides the variation of α^* , which in the present case corresponds approximately to a sideslip angle ($\alpha^* \approx \beta$). The drag and lift forces of the cluster and AUV are reported in Fig. 11(a) and (b). Figure 12(a) and (b) report the evolution of the lift forces and moments for the cluster system and the four AUVs, respectively, each one expressed in its body frame. As already highlighted, the drag and lift forces on the cluster are the sum of the drag and lift forces on the four AUVs. In this case the angle of attack α^* illustrated in Fig. 10(b), characterized by a not null sideslip angle, gives rise to a lift contribution that generate first additional sway, heave, pitch, and yaw motions, and then additional surge and roll motions. The resulting vehicle attitude and restoring forces and moments are illustrated in Fig. 13.

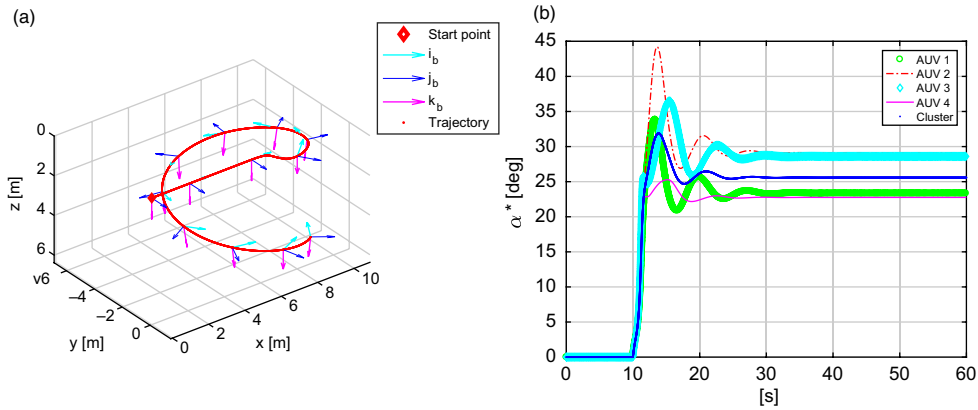


Fig. 10. (a) Trajectory of the 4 *Folaga* cluster. (b) Evolution of the angle of attack α^* of the 4-*Folaga* cluster system and the four *Folaga*-AUVs while performing trajectory

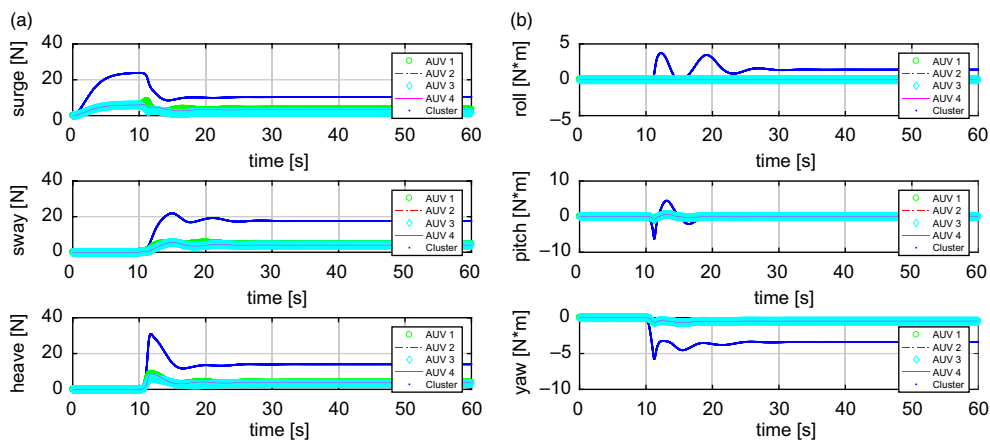


Fig. 11. (a) Drag forces of the 4-*Folaga* cluster system and the four *Folaga*-AUVs while performing trajectory in Fig. 10. (b) Drag moments of the 4-*Folaga* cluster system and the four *Folaga*-AUVs while performing trajectory in Fig. 10.

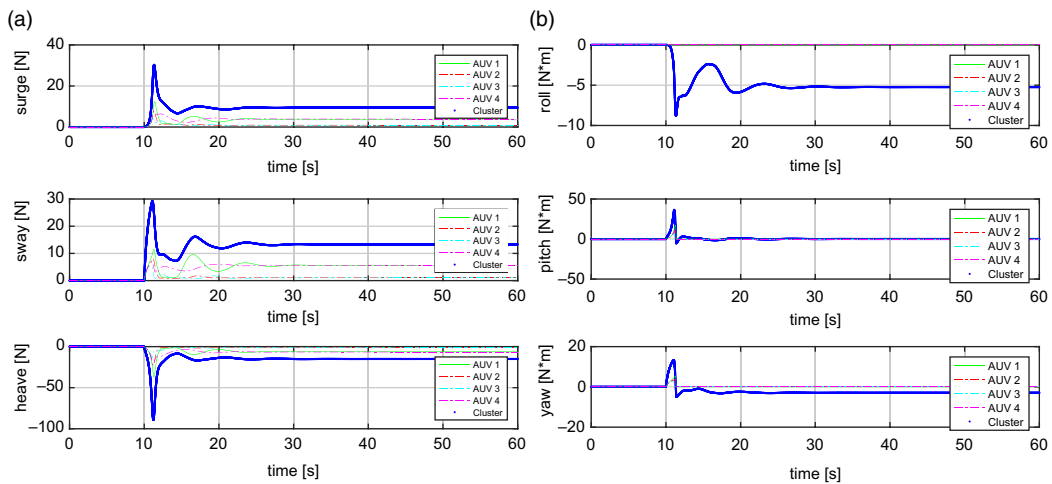


Fig. 12. (a) Lift forces of the 4 *Folaga* cluster system and the four *Folaga*-AUVs while performing trajectory in Fig. 10. (b) Lift moments of the 4 *Folaga* cluster system and the four *Folaga*-AUVs while performing trajectory in Fig. 10.

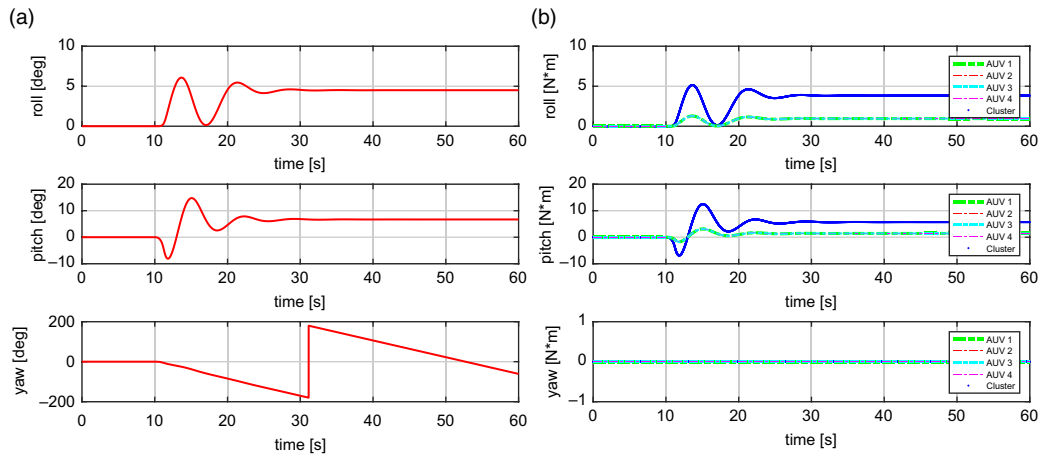


Fig. 13. (a) Attitude of the 4-Folaga cluster system while performing trajectory in Fig. 10. (b) Restoring moments of the 4-Folaga cluster system and the four Folaga-AUVs while performing the same trajectory

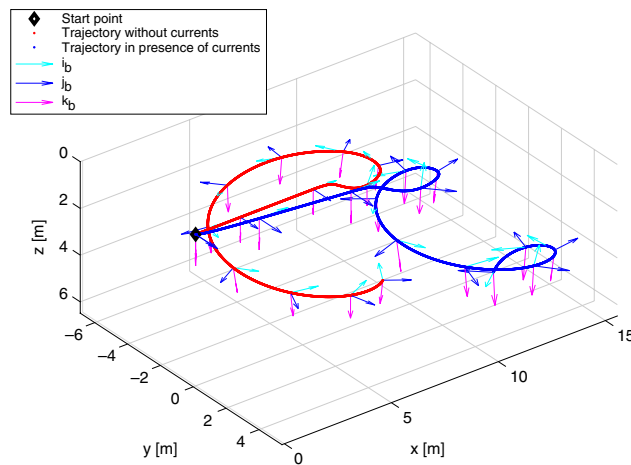


Fig. 14. Trajectory of cluster without currents (red) and in the presence of ocean currents (blue).

The same simulation (i.e., same inputs) is repeated in the presence of a constant and irrotational ocean current in the inertial NED frame, namely with ${}^0\mathbf{v}_{f/o} = [0.1 \ 0.1 \ 0]^T$ [m/s], and ${}^0\boldsymbol{\omega}_{f/o} = \mathbf{0}_{1 \times 3}$ [rad/s]. The initial condition of the cluster relative velocity is assumed to be null, ${}^0\mathbf{v}_{c/o} = \mathbf{0}_{1 \times 6}$. Consequently, the two cases differ in the kinematics only as illustrated in Fig. 14.

5. Conclusions

A modeling approach has been developed to compute the lumped parameter hydrodynamic derivative matrices for a generic multi-hull underwater vehicle. In particular, its dynamic model has been built on the knowledge of the single basic bodies exploiting a specific multi-body composition approach. This allows the derivation of a dynamic–hydrodynamic model for the whole multi-body system without solving explicitly the constraints imposed by the rigid connections. The present paper provides a generic framework to model modular underwater vehicles. It presents the advantage to simplify the control system design for the overall system and potentially improve its performance. Moreover, it offers a method allowing to perform a dynamic analysis before the cluster vehicle is actually built, under the hypothesis of a sufficiently large separation between the bodies. For example, when larger vehicles are realized by means of a cluster of existing robots, performance and suitability of different geometric configurations can be numerically estimated as soon as the dynamic model is available. Possible control method that could also benefit from the proposed dynamic modeling approach may include path-following controllers, task priority-based controllers, formation control tasks, or inspection tasks. Finally, numerical simulations have been presented applying the proposed

methodology to a hypothetical cluster composed of four AUVs, whose models were already studied in the past.

Acknowledgments

This work was partially supported by the European Union's Horizon 2020 research and innovation program under the project ROBUST: Robot subsea exploration technologies, grant agreement N.690416 (call H2020-SC5-2015-one-stage). The authors would like to warmly thank Prof. Enrico Simetti from the University of Genova (ISME node) and Graal Tech s.r.l. for the useful discussions and the data relative to the ROBUST UVMS platform.

References

1. G. Antonelli, *Underwater Robots*, vol. 96. Springer Tracts in Advanced Robotics (Springer International Publishing, Switzerland, 2014).
2. T. I. Fossen, *Handbook of Marine Craft Hydrodynamics and Motion Control* (John Wiley & Sons, Ltd., United Kingdom, 2011).
3. P. Cardenas and E. A. de Barros, "Estimation of AUV hydrodynamic coefficients using analytical and system identification approaches," *IEEE J. Ocean. Eng.*, 1–20 (2019).
4. M. Caccia, G. Indiveri and G. Veruggio, "Modelling and identification of open-frame variable configuration unmanned underwater vehicles," *IEEE J. Ocean. Eng.* **5**, 227–240 (2000).
5. Z. Peng, J. Wang and Q.-L. Han, "Path-following control of autonomous underwater vehicles subject to velocity and input constraints via neurodynamic optimization," *IEEE Trans. Ind. Electron.* **66**(11), 8724–8732 (2018).
6. J. W. Kamman and R. L. Huston. "Modelling of submerged cable dynamics," *Comput. Struct.* **20**(1), 623–629 (1985). Special Issue: Advances and Trends in Structures and Dynamics.
7. J. W. Kamman and R. L. Huston, "Multibody dynamics modeling of variable length cable systems," *Multibody Syst. Dyn.* **5**(3), 211–221 (2001).
8. P. Abreu, H. Morishita, A. Pascoal, J. Ribeiro and H. Silva, "Marine Vehicles with Streamers for Geotechnical Surveys: Modeling, Positioning, and Control," **In: Proceedings of the 10th IFAC Conference on Control Applications in Marine Systems, CAMS 2016**, vol. 49 (V. Hassani, ed.) (Elsevier, Netherlands, 2016), pp. 458–464.
9. H. Huang, Q. Tang, H. Li, L. Liang, W. Li and Y. Pang, "Vehicle-manipulator system dynamic modeling and control for underwater autonomous manipulation," *Multibody Syst. Dyn.* **41**(2), 125–147 (2017). ISSN: 1573-272X.
10. Y. Ke, W. Xu-yang, G. Tong and W. Chao, "A dynamic model of an underwater quadruped walking robot using Kane's method," *J. Shanghai Jiaotong Univ. (Sci.)* **19**(2), 160–168 (2014).
11. Y. Ke, W. Xuyang, G. Tong and W. Chao, "A Dynamic Model of ROV with a Robotic Manipulator Using Kane's Method," **In: 2013 Fifth International Conference on Measuring Technology and Mechatronics Automation**, Hong Kong (2013) pp. 9–12.
12. J. Park and N. Kim, "Dynamics modeling of a semi-submersible autonomous underwater vehicle with a towfish towed by a cable," *Int. J. Naval Archit. Ocean Eng.* **7**(2), 409–425 (2015).
13. H. Zhang and S. Wang, "Modelling and Analysis of an Autonomous Underwater Vehicle via Multibody System Dynamics," *Proceedings of the 12th IFToMM World Congress*, Besancon, France (2007) pp. 1–6.
14. M. C. Nielsen, O. A. Eidsvik, M. Blanke and I. Schjøberg, "Validation of multi-body modelling methodology for reconfigurable underwater robots," *OCEANS 2016 MTS/IEEE Monterey*, Monterey, CA, USA (2016) pp. 1–8.
15. M. C. Nielsen, M. Blanke and I. Schjøberg, "Efficient Modelling Methodology for Reconfigurable Underwater Robots," *Proceedings of the 10th IFAC Conference on Control Applications in Marine Systems, CAMS 2016*, Trondheim, Norway, vol. 49 (2016) pp. 74–80.
16. M. C. Nielsen, O. A. Eidsvik, M. Blanke and I. Schjøberg, "Constrained multi-body dynamics for modular underwater robots — theory and experiments," *Ocean Engineering* **149**, 358–372 (2018).
17. K. Yang, "Dynamic model and CPG network generation of the underwater self-reconfigurable robot," *Adv. Robot.* **30**(14), 925–937 (2016).
18. F. E. Udwardia and A. D. Schutte, "A unified approach to rigid body rotational dynamics and control," *Proc. Roy. Soc. London A Math. Phys. Eng. Sci.* **468**(2138), 395–414 (2011).
19. E. Simetti, F. Wanderlingh, G. Casalino, G. Indiveri and G. Antonelli, "Robust project: Control framework for deep sea mining exploration," *OCEANS 2017*, Anchorage (2017) pp. 1–5.
20. R. Ingrosso, D. De Palma, G. Indiveri and G. Avanzini, "Preliminary Results of a Dynamic Modelling Approach for Underwater Multi-Hull Vehicles," *Proceedings of the 11th IFAC Conference on Control Applications in Marine Systems, Robotics, and Vehicles – CAMS 2018* (N. Mišković, ed.), Opatija, Croatia, vol. 51 (2018) pp. 86–91.
21. T. I. Fossen, *Guidance and Control of Ocean Vehicles* (John Wiley & Sons Inc., United Kingdom, 1994).
22. B. Siciliano and O. Khatib, *Handbook of Robotics* (Springer-Verlag, Berlin, Heidelberg, 2008).
23. T. I. Fossen, "How to Incorporate Wind, Waves and Ocean Currents in the Marine Craft Equations of Motion," *9th IFAC Conference on Manoeuvring and Control of Marine Craft*, Arenzano, Italy, vol. 45 (2012) pp. 126–131.

24. T. I. Fossen, *Marine Control Systems: Guidance, Navigation and Control of Ships, Rigs and Underwater Vehicles* (Marine Cybernetics, Trondheim, Norway, 2002).
25. S. F. Hoerner and H. V. Borst, *Fluid-Dynamic Lift, Practical Information on Aerodynamic and Hydrodynamic Lift* (Mrs. Liselotte A. Hoerner, NASA STI/ Recon Technical Report A 1985).
26. J. N. Newman, *Marine Hydrodynamics* (MIT Press, Cambridge, Massachusetts, 1977).
27. A. Alvarez, A. Caffaz, A. Caiti, G. Casalino, L. Gualdesi, A. Turetta and R. Viviani, "Folaga: A low-cost autonomous underwater vehicle combining glider and AUV capabilities," *Ocean Eng.* **36**, 24–38 (2009).
28. A. Canepa, Guida e controllo di veicoli sottomarini autonomi. *Master's thesis*, University of Genova, Informatic Engineering (March 2011).

Appendix

A. Derivation of Dynamic Pressure Generalized Forces on k -th Vehicle (25)

The dynamic pressure forces and moments acting on the k -th vehicle expressed in its local body frame $\{k\}$ are given by (24):

$${}^k_{p_k} \boldsymbol{\tau}_{dp_k} = -M_{A_k} \frac{d}{dt} {}^k \mathbf{v}_{p_k/o} - C_{A_k} ({}^k \mathbf{v}_{p_k/o}) {}^k \mathbf{v}_{p_k/o}.$$

As highlighted in Section 2.4, these actions can be projected in the cluster-fixed reference frame $\{b\}$ by means of the matrix ${}^b\bar{R}_k$:

$$\begin{aligned} {}^b_{p_k} \boldsymbol{\tau}_{dp_k} &= {}^b\bar{R}_k {}^k_{p_k} \boldsymbol{\tau}_{dp_k} = {}^b\bar{R}_k \{-M_{A_k} {}^k\bar{R}_b \frac{d}{dt} {}^b \mathbf{v}_{p_k/o} - C_{A_k} ({}^k \mathbf{v}_{p_k/o}) {}^k\bar{R}_b {}^b \mathbf{v}_{p_k/o}\} = \\ &= -({}^b\bar{R}_k M_{A_k} {}^k\bar{R}_b) \frac{d}{dt} {}^b \mathbf{v}_{p_k/o} - {}^b\bar{R}_k \begin{bmatrix} S({}^k \boldsymbol{\omega}_{b/o}) & 0_{3 \times 3} \\ S({}^k \mathbf{v}_{p_k/o}) & -S({}^k \boldsymbol{\omega}_{b/o}) \end{bmatrix} M_{A_k} {}^k\bar{R}_b {}^b \mathbf{v}_{p_k/o} = \\ &= -({}^b\bar{R}_k M_{A_k} {}^k\bar{R}_b) \frac{d}{dt} {}^b \mathbf{v}_{p_k/o} - {}^b\bar{R}_k \begin{bmatrix} S({}^k \boldsymbol{\omega}_{b/o}) & 0_{3 \times 3} \\ S({}^k \mathbf{v}_{p_k/o}) & -S({}^k \boldsymbol{\omega}_{b/o}) \end{bmatrix} {}^k\bar{R}_b {}^b\bar{R}_k M_{A_k} {}^k\bar{R}_b {}^b \mathbf{v}_{p_k/o}. \end{aligned} \tag{A1}$$

Exploiting the following property of a generic rotation matrix R

$$RS(\mathbf{x})R^T = S(R\mathbf{x}) \forall R \in SO(3), \mathbf{x} \in \mathbb{R}^3,$$

the (A1) yields:

$$\begin{aligned} {}^b_{p_k} \boldsymbol{\tau}_{dp_k} &= -({}^b\bar{R}_k M_{A_k} {}^k\bar{R}_b) \frac{d}{dt} {}^b \mathbf{v}_{p_k/o} - \begin{bmatrix} S({}^b R_k {}^k \boldsymbol{\omega}_{b/o}) & 0_{3 \times 3} \\ S({}^b R_k {}^k \mathbf{v}_{p_k/o}) & -S({}^b R_k {}^k \boldsymbol{\omega}_{b/o}) \end{bmatrix} {}^b\bar{R}_k M_{A_k} {}^k\bar{R}_b {}^b \mathbf{v}_{p_k/o} = \\ &= -({}^b\bar{R}_k M_{A_k} {}^k\bar{R}_b) \frac{d}{dt} {}^b \mathbf{v}_{p_k/o} - \begin{bmatrix} S({}^b \boldsymbol{\omega}_{b/o}) & 0_{3 \times 3} \\ S({}^b \mathbf{v}_{p_k/o}) & -S({}^b \boldsymbol{\omega}_{b/o}) \end{bmatrix} ({}^b\bar{R}_k M_{A_k} {}^k\bar{R}_b) {}^b \mathbf{v}_{p_k/o}. \end{aligned} \tag{A2}$$

Hence, the Eq. (A2) becomes:

$${}^b_{p_k} \boldsymbol{\tau}_{dp_k} = -\bar{M}_{A_k} \frac{d}{dt} {}^b \mathbf{v}_{p_k/o} - \bar{C}_{A_k} ({}^b \mathbf{v}_{p_k/o}) \bar{M}_{A_k} {}^b \mathbf{v}_{p_k/o}, \tag{A3}$$

where \bar{M}_{A_k} and $\bar{C}_{A_k} ({}^b \mathbf{v}_{p_k/o})$ are defined as:

$$\bar{M}_{A_k} = {}^b\bar{R}_k M_{A_k} {}^k\bar{R}_b, \tag{A4}$$

$$\bar{C}_{A_k} ({}^b \mathbf{v}_{p_k/o}) = \begin{bmatrix} S({}^b \boldsymbol{\omega}_{b/o}) & 0_{3 \times 3} \\ S({}^b \mathbf{v}_{p_k/o}) & -S({}^b \boldsymbol{\omega}_{b/o}) \end{bmatrix} \bar{M}_{A_k}. \tag{A5}$$

Now, exploiting the transformation between ${}^b \mathbf{v}_{p_k/o}$ and ${}^b \mathbf{v}_{c/o}$ defined in (7), Eq. (A3) can be rewritten as:

$${}^b_{p_k} \boldsymbol{\tau}_{dp_k} = -\bar{M}_{A_k} T({}^b \mathbf{r}_{c,p_k}) \frac{d}{dt} {}^b \mathbf{v}_{c/o} - \bar{C}_{A_k} (T({}^b \mathbf{r}_{c,p_k}) {}^b \mathbf{v}_{c/o}) T({}^b \mathbf{r}_{c,p_k}) {}^b \mathbf{v}_{c/o}. \tag{A6}$$

Finally, the pole for moments can be moved from p_k to c by means of the transformation matrix $T({}^b\mathbf{r}_{c,p_k})$:

$${}^b_c\boldsymbol{\tau}_{dp_k} = -T^\top({}^b\mathbf{r}_{c,p_k}) \bar{M}_{A_k} T({}^b\mathbf{r}_{c,p_k}) \frac{d}{dt} {}^b\mathbf{v}_{c/o} - T^\top({}^b\mathbf{r}_{c,p_k}) \bar{C}_{A_k}({}^b\mathbf{v}_{c/o}) T({}^b\mathbf{r}_{c,p_k}) {}^b\mathbf{v}_{c/o}, \tag{A7}$$

where $\bar{C}_{A_k}({}^b\mathbf{v}_{c/o})$ is given by:

$$\bar{C}_{A_k}({}^b\mathbf{v}_{c/o}) = \begin{bmatrix} S({}^b\boldsymbol{\omega}_{b/0}) & 0_{3 \times 3} \\ S({}^b\mathbf{v}_{c/o} + {}^b\boldsymbol{\omega}_{b/0} \times {}^b\mathbf{r}_{c,p_k}) & S({}^b\boldsymbol{\omega}_{b/0}) \end{bmatrix} \bar{M}_{A_k}. \tag{A8}$$

B. Derivation of Drag Generalized Forces on k -th Vehicle (43)

The hydrodynamic drag forces acting on the k -th vehicle expressed in its local body frame $\{k\}$ are given by:

$${}^k_{p_k}\boldsymbol{\tau}_{dragk} = -{}^k_{p_k}D_k({}^k\mathbf{v}_{p_k/o}) {}^k\mathbf{v}_{p_k/o}, \tag{A9}$$

where

$${}^k_{p_k}D_k({}^k\mathbf{v}_{p_k/o}) = {}^k_{p_k}D_{k_{lin}} + {}^k_{p_k}D_{k_{quad}}({}^k\mathbf{v}_{p_k/o}). \tag{A10}$$

Following the procedure illustrated in 2.4, the damping forces ${}^k_{p_k}\boldsymbol{\tau}_{dragk}$ can be expressed in the frame $\{b\}$ leading to:

$${}^b_{p_k}\boldsymbol{\tau}_{dragk} = {}^b\bar{R}_k {}^k_{p_k}\boldsymbol{\tau}_{dragk} = -{}^b\bar{R}_k {}^k_{p_k}D_k({}^k\mathbf{v}_{p_k/o}) {}^k\mathbf{v}_{p_k/o} = \tag{A11}$$

$$= -{}^b\bar{R}_k {}^k_{p_k}D_k({}^k\mathbf{v}_{p_k/o}) {}^k\bar{R}_b {}^b\mathbf{v}_{p_k/o}. \tag{A12}$$

Now, the pole for moments can be moved from p_k to c by means of the transformation matrix $T({}^b\mathbf{r}_{c,p_k})$:

$${}^b_c\boldsymbol{\tau}_{dragk} = T^\top({}^b\mathbf{r}_{c,p_k}) {}^b_{p_k}\boldsymbol{\tau}_{dragk} = -T^\top({}^b\mathbf{r}_{c,p_k}) {}^b\bar{R}_k {}^k_{p_k}D_k({}^k\mathbf{v}_{p_k/o}) {}^k\bar{R}_b {}^b\mathbf{v}_{p_k/o}. \tag{A13}$$

Exploiting the transformation between ${}^b\mathbf{v}_{p_k/o}$ and ${}^b\mathbf{v}_{c/o}$ defined in (7), Eq. (A13) becomes:

$${}^b_c\boldsymbol{\tau}_{dragk} = -T^\top({}^b\mathbf{r}_{c,p_k}) {}^b\bar{R}_k {}^k_{p_k}D_k({}^k\mathbf{v}_{p_k/o}) {}^k\bar{R}_b T({}^b\mathbf{r}_{c,p_k}) {}^b\mathbf{v}_{c/o}. \tag{A14}$$

Finally, Eq. (A13) can be rewritten as:

$${}^b_c\boldsymbol{\tau}_{dragk} = -T^\top({}^b\mathbf{r}_{c,p_k}) {}^b\bar{D}_k({}^b\mathbf{v}_{c/o}) T({}^b\mathbf{r}_{c,p_k}) {}^b\mathbf{v}_{c/o}, \tag{A15}$$

having defined ${}^b\bar{D}_k({}^b\mathbf{v}_{c/o})$ as:

$${}^b\bar{D}_k({}^b\mathbf{v}_{c/o}) = {}^b\bar{R}_k {}^k_{p_k}D_k({}^k\mathbf{v}_{p_k/o}) {}^k\bar{R}_b = {}^b\bar{R}_k {}^k_{p_k}D_k({}^k\bar{R}_b T({}^b\mathbf{r}_{c,p_k}) {}^b\mathbf{v}_{c/o}) {}^k\bar{R}_b. \tag{A16}$$